Inverse Design Method for Wing of Supersonic Transport

Shinkyu Jeong*, Shigeru Obayashi*, and Kazuhiro Nakahashi♣
Tohoku University, 980-77, Sendai, Japan
Ph:81-22-217-6981, Fax:81-22-217-6979
E-mail:jeong2@ad.mech.tohoku.ac.jp

Kisa Matsushima**
Fujitsu Limited, Chiba 261, Japan
Ph:81-43-299-3211, Fax:81-43-299-3013

Toshiyuki Iwamiya***
National Aerospace Laboratory, Chofu, Tokyo 182, Japan
Ph:81-422-47-5911, Fax:81-422-8569

Abstract

The inverse design method for supersonic transport is developed. This method utilize Takanashi's residual-correction concept which is used in the transonic inverse problem. The difference between the computed pressure distribution of given wing and the prescribed target pressure distribution is iteratively reduced by solving the integrodifferential form of linearized small perturbation(LSP) equation. The pressure distribution is computed by Euler/Navier-Stokes equation. The numerical result show the possibility of using this method to the design of SST.

Introduction

The next generation supersonic transport (SST) is under consideration today, since the Concorde has been in service for 20 years and not fully successful in the economic sense. There are many researches on this field now in the United State, Europe, and Japan. To guarantee its economic success, the next generation SST is required to have higher L/D than that of the Concorde. To achieve this goal, development of a new design technique for supersonic wings is of strong interest. For the transonic wing design, Takanashi[1] proposed an inverse method which uses the "residual-correction" concept and showed successful design results[2]. In this paper, this inverse method is extended to the supersonic wing design. In the supersonic flow, the governing equation can be Linearized. So the integration becomes simpler than that of the transonic case, but the integration region must be selected carefully because the region that contributes to the point on the wing surface is limited to Mach foregone. The sample design results of airfoils and wings confirm the validity of the present method.

Design Procedure

The inverse design method seeks a geometry that materializes the specified pressure distribution. With this target pressure distribution specified, the corresponding geometry can be obtained as follows. First, the performance of the initial geometry is analyzed by the Euler/Navier-Stokes code and the difference between this computed pressure distribution and the target pressure distribution is calculated. If two pressure

---

* Graduate Student, Dept. of Aerodynamics & Space Engineering,
* Associate Professor, Dept. of Aeronautics & Space Engineering, Senior Member AIAA
♣Professor, Dept. of Aeronautics & Space Engineering, Associate Fellow AIAA
** Research Scientist, Supercomputer Systems Engineering Division, Member AIAA
*** Head of Applied Math. Lab., Computer Science Division

distributions coincide with each other, the initial geometry is the final geometry. If not, a geometry correction is executed by using the solution of the inverse Linearized small perturbation (LSP) equation. For this new geometry, the performance is analyzed and the difference from two pressure distributions is calculated. This process is repeated until the difference of pressure distributions is eliminated. Through this process, the geometry corresponding to the prescribed pressure distribution can be obtained. Figure 1 shows the flowchart of the above procedure.

Integral Formulation for Inverse Method

In a supersonic flow, the small perturbation potential equation can be written in the Linearized form as

$$\left(M_\infty^2 - 1\right)\bar{\phi}_{\bar{x}\bar{x}} - \bar{\phi}_{\bar{y}\bar{y}} - \bar{\phi}_{\bar{z}\bar{z}} = 0 \tag{1}$$

and pressure coefficients on wing surfaces and the tangency conditions can be written as

$$C_{p\pm}\left(\bar{x},\bar{y}\right) = -2\bar{\phi}_{\bar{x}}\left(\bar{x},\bar{y},\pm 0\right) \tag{2}$$

$$\frac{\partial \bar{z}_\pm\left(\bar{x},\bar{y}\right)}{\partial \bar{x}} = \bar{\phi}_{\bar{z}}\left(\bar{x},\bar{y},\pm 0\right) \tag{3}$$

where the subscript '±' denotes the upper and lower surfaces of the wing. For the convenience of the computation, a Prandtl-Glauert transformation is used in the above equations as

$$x = \bar{x},\ y = \beta\bar{y},\ z = \beta\bar{z},\ \phi\left(x,y,x\right) = \left(\frac{K}{\beta^2}\right)\bar{\phi}\left(\bar{x},\bar{y},\bar{z}\right) \tag{4}$$

where

$$\beta = \sqrt{M_\infty^2 - 1},\ K = \left(1+\gamma\right)M_\infty^2 \tag{5}$$

The transformed equations are written as

$$\phi_{xx} - \phi_{yy} - \phi_{zz} = 0 \tag{6}$$

$$C_{p\pm}\left(x,\frac{y}{\beta}\right) = -2\frac{\beta^2}{K}\phi_x\left(x,y,\pm 0\right) \tag{7}$$

$$\frac{\partial z_\pm\left(x,y\right)}{\partial x} = \frac{\beta^3}{K}\phi_z\left(x,y,\pm 0\right) \tag{8}$$

Suppose the solution of Eq. (6) for the initial geometry z(x, y) is given as $\phi(x, y, z)$. The perturbation solution $\phi(x, y, z)+\Delta\phi(x, y, z)$ should satisfy

$$\left(\phi_{xx} + \Delta\phi_{xx}\right) - \left(\phi_{yy} + \Delta\phi_{yy}\right) - \left(\phi_{zz} + \Delta\phi_{zz}\right) = 0 \tag{9}$$

$$C_{p\pm}\left(x,\frac{y}{\beta}\right) + \Delta C_{p\pm}\left(x,\frac{y}{\beta}\right) = -2\frac{\beta^2}{K}\left[\phi_x\left(x,y,\pm 0\right) + \Delta\phi_x\left(x,y,\pm 0\right)\right] \tag{10}$$

$$\frac{\partial z_\pm\left(x,y\right)}{\partial x} + \frac{\partial \Delta\phi\left(x,y\right)}{\partial x} = \frac{\beta^3}{K}\left[\phi_z\left(x,y,\pm 0\right) + \Delta\phi_z\left(x,y,\pm 0\right)\right] \tag{11}$$

By subtracting Eqs. (6) - (8) from Eqs. (9) - (11), the perturbation equations are obtained as

$$\Delta\phi_{xx} - \Delta\phi_{yy} - \Delta\phi_{zz} = 0 \tag{12}$$

$$\Delta C_{p\pm}\left(x,\frac{y}{\beta}\right) = -2\frac{\beta^2}{K}\Delta\phi_x\left(x,y,\pm 0\right) \tag{13}$$

$$\frac{\partial \Delta\phi\left(x,y\right)}{\partial x} = \frac{\beta^3}{K}\Delta\phi_z\left(x,y,\pm 0\right) \tag{14}$$

The solution of Eq. (12), $\Delta\phi$, can be derived by means of Green's theorem[3),4)]:

$$\begin{aligned}\Delta\phi(x,y,z) &= -\frac{1}{2\pi}\frac{\partial}{\partial x}\iint_{\tau_1}\left[\left(\Delta\phi_\zeta(\xi,\eta,+0) - \Delta\phi_\zeta(\xi,\eta,-0)\right)\times\varphi(x,y,z;\xi,\eta,0)\right]d\xi d\eta \\ &+ \frac{1}{2\pi}\frac{\partial}{\partial x}\iint_{\tau_1}\left[\left(\Delta\phi(\xi,\eta,+0) - \Delta\phi(\xi,\eta,-0)\right)\times\varphi_\zeta(x,y,z;\xi,\eta,0)\right]d\xi d\eta\end{aligned} \tag{15}$$

where

$$\varphi(x,y,z;\xi,\eta,\zeta)=\arccosh\frac{x-\xi}{\sqrt{(y-\eta)^2+(z-\zeta)^2}} \quad (16)$$

The area is that part of the z = 0 plane contained within the Mach forecone from the point (x, y, z), that is, the area bounded by the line $\xi = -\infty$ and the hyperbola $(x-\xi)^2-(y-\eta)^2-(z-\zeta)^2=0$

Since Eq. (15) includes improper integrals in it, the differentiation cannot move through the integral signs. This obstacle can be eliminated by using Hadamard's "finite part"[5]. To utilize the pressure distributions as a boundary condition, Eq. (15) is differentiated with respect to x and by adding the values of the resulting $\Delta\phi_x(x, y, z)$ at $z = +0$ and $z = -0$, we obtain

$$\Delta u_s(x,y)=-\Delta w_s(x,y)+\frac{1}{\pi}\iint_{\tau_1}\frac{(x-\xi)\Delta w_s(\xi,\eta)}{\sqrt{(x-\xi)^2-(y-\eta)^2}^3}d\xi d\eta \quad (17)$$

$$\Delta u_s(x,y)=\Delta\phi_x(x,y,+0)+\Delta\phi_x(x,y,-0) \quad (18)$$

$$\Delta w_s(x,y)=\Delta\phi_z(x,y,+0)-\Delta\phi_z(x,y,-0) \quad (19)$$

Similarly, differentiating both sides of Eq. (15) with respect to z and adding the values of the resulting $\Delta\phi_z(x, y, z)$ at $z = +0$ and $z = -0$.

$$\Delta w_a=-\Delta u_a(x,y)+\frac{1}{\pi}\iint_{\tau_1}\frac{(x-\xi)\Delta u_a(x,y)}{(y-\eta)^2\sqrt{(x-\xi)^2-(y-\eta)^2}}d\xi d\eta \quad (20)$$

$$\Delta u_s(x,y)=\Delta\phi_x(x,y,+0)-\Delta\phi_x(x,y,-0) \quad (21)$$

$$\Delta w_a(x,y)=\Delta\phi_z(x,y,+0)+\Delta\phi_z(x,y,-0) \quad (22)$$

By solving Eqs. (17) and (20) with the boundary conditions Δu_s and Δu_a, the geometry terms Δw_s and Δw_a can be obtained. As defined in Eqs. (19) and (22), $\Delta w_s(x, y)$ and $\Delta w_a(x, y)$ represent the derivatives of thickness and camber correction, respectively. So the value of geometry correction can be computed by performing the numerical integration in the x direction.

$$\Delta z_{\pm}(x,y)=\frac{1}{2}\int_{L.E}^{x}\Delta w_a(\xi,y)d\xi\pm\frac{1}{2}\int_{L.E}^{x}\Delta w_s(\xi,y)d\xi \quad (23)$$

Results

To confirm the validity of the present formulation of the inverse method for the supersonic wing design, numerical calculations are performed for two-dimensional airfoils and the three-dimensional wing.

Case1: Two-Dimensional Airfoil Designs

As an analysis code, a Navier-Stokes code. This code utilizes a TVD upwind scheme for the spatial discretization of the convective terms and the LU-SGS method for the time integration. The computational grid is generated by an algebraic grid generation code.

NACA1204 and NACA0003 are selected as reference airfoils. First, NACA1204 airfoil is designated as a target airfoil. By taking its pressure distribution as a target, the present inverse design code is applied to reconstruct its shape, starting from NACA 0003 airfoil. The flow condition is assumed as M = 2.0, $Re=1.45\times10^7$ and $\alpha = 0°$. The design result is shown in Figure 2. Both target and computed geometries and pressure distributions coincide with each other.

NACA66003 is selected as a reference airfoil for the second test case. First, pressure distributions of this airfoil are calculated at both 0° and 2° angles of attack and the pressure distribution at 2° angle of attack is designated as a target. Design procedure starts with the pressure distribution over

NACA66003 airfoil at 0° angle of attack. As shown in Fig. 3, the designed airfoil inclined 2° degrees as specified in the target pressure distribution.

Case 2: Three-Dimensional Wing Design

The Euler code is used as an analysis code for the wing design. The spatial discretization and time integral technique are the same scheme as used in the two dimensional airfoil design. The initial and target wing geometries are made for the same warp geometry by using NACA0003 and NACA66003 airfoils, respectively. The initial wing geometry is shown in figure 4. The pressure distribution of the wing that use NACA66003 is designated as target. The flow conditions is set to M = 2.0, Re=1.45×10^7 and α= 2°. Pressure distributions of initial, target, and designed wing at the 20% and 50% spanwise sections are shown in figures 5 and 6. As shown in the figures, the pressure distributions of the designed wing are nearly converged to the target.

Conclusion

In this investigation, Takanashi's inverse design method is extended to supersonic airfoil design. The numerical results show the possibility of using this method to the design of supersonic transport. When using the inverse method as a design tool, designers must translate their design criteria of supersonic wings into target pressure distributions. The determination of optimal target pressure distributions will be studied in future.

References

1. Takanashi, S., "Iterative Three-Dimensional Transonic Wing Design Using Integral Equations," *Journal of aircraft*, Vol. 22, No. 8, pp.655-660, Aug. 1985.

2. Obayashi, S., Jeong, S. K. and Matsuo, Y., "Inverse Optimization Method for Blunt-Trailing-Edge Airfoils," Proc. of 15th International Conference on Numerical Methods in Fluid Dynamics, pp.162-163, June 1996.

3. Lomax, H., Heaslet, M. A. and Franklyn, B. Fuller, "Integrals and Integral Equation in Linearized Wing Theory," NACA Rep. 1054, 1951.

4. Heaslet, M. A., Lomax, H., and Jones, A. L., "Volterra's Solution of the Wave Equation as Applied to Three-Dimensional Supersonic Airfoil Problem," NACA Rep. 889, 1947. (Formerly NACA TN 1412.)

5. Hadamard, J., "Lectures on Cauchy's Problem in Linear Partial Differential Equations," Yale University Press, 1928.

6. Carlson, H. W. and Middleton, W. D., "A Numerical Method for Design of Camber Surfaces of Supersonic Wings with Arbitrary Planforms," NASA TN D-2341, 1964

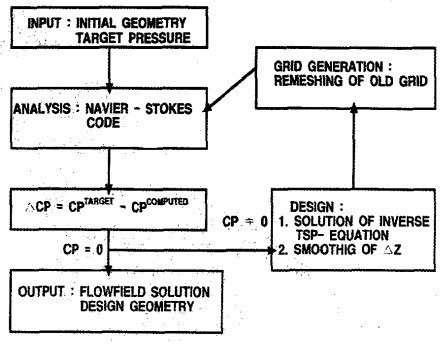

Figure1. Flowchart of inverse design procedure

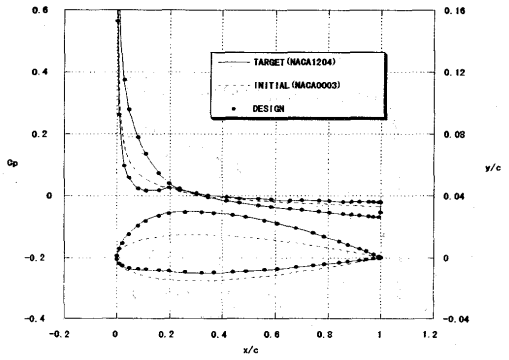

Figure 2. Inverse design result and comparison of pressure distributions

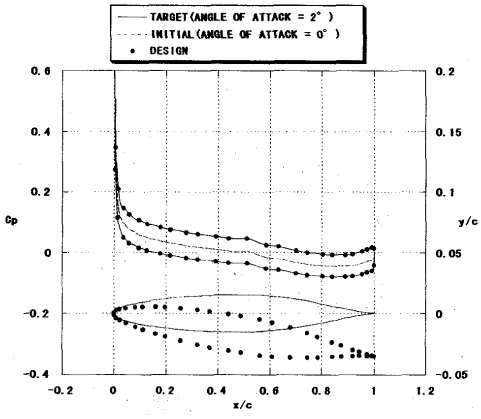

Figure 3. Inverse design result and comparison of pressure distributions

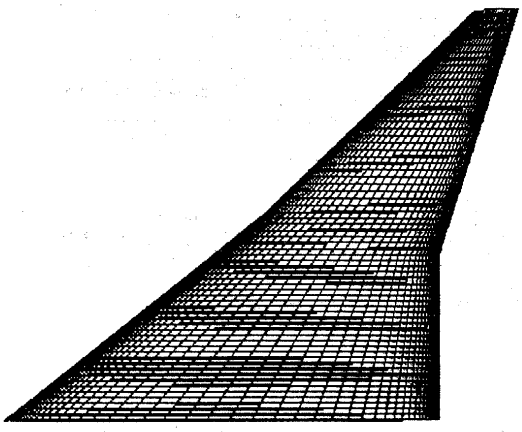

Figure 4. The wing geometry of initial wing

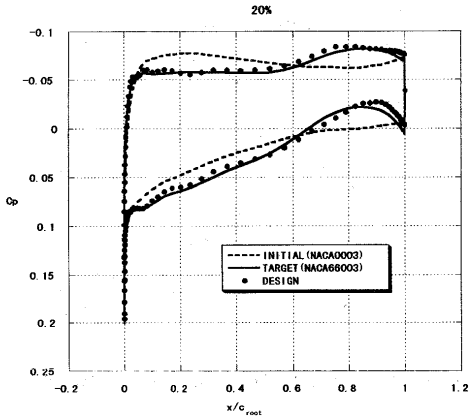

Figure 5. Comparison of surface pressure distributions (y/l=20%)

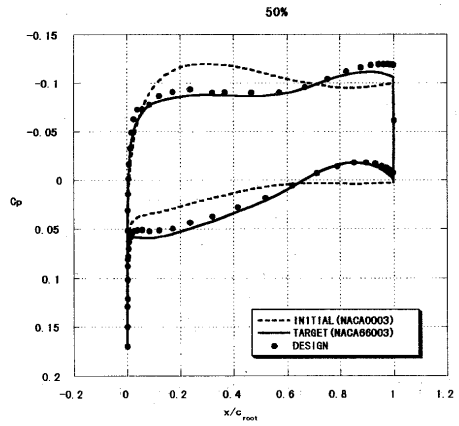

Figure 6. Comparison of surface pressure distributions (y/l=50%)